Relativistic corrections in the ground and excited states of positronic beryllium

Dmitry Tumakov [1,2,*] Pavel Rzhevskii [1,†] Toreniyaz Shomenov [1,‡] and Sergiy Bubin [1,§]

[1]*Department of Physics, Nazarbayev University, Astana 010000, Kazakhstan*
[2]*I. Institute for Theoretical Physics, Universität Hamburg, Hamburg 22607, Germany*

Positron binding to neutral atoms, which to this day have not been detected experimentally, is thought to be rather weak. According to a few reliable nonrelativistic calculations reported previously, the positron affinity for small atoms, even if it happens to be positive, is predicted to be very small in magnitude, of the order of just few millihartrees (<0.1 eV). In this work, we used a highly accurate variational expansion in terms of explicitly correlated Gaussians to investigate how relativistic effects may affect the stability of bound states of positrons with atoms. We performed calculations of positronic beryllium, e^+[Be], in its ground singlet S and excited triplet S and P states, all of which are bound. According to our findings, neither the inclusion of scalar relativistic nor spin-dependent corrections alters the predictions regarding the existence of the bound states. When leading-order relativistic effects are taken into account, positron affinities change only by 2.2% or less. Notably, this is so even for the triplet P state of positronic beryllium, where the spin-orbit correction is not at all canceled out when the energy difference with the parent system is computed.

I. INTRODUCTION

The study of matter and antimatter interaction is of great importance for understanding the fundamental nature of the universe and its origins. Simple quantum systems containing a positron represent, perhaps, the simplest and most tractable realization of this interaction. In fact, the possibility of a positron attracting to one or two electrons and forming a bound state has been considered for a long time. The first speculation of it can be traced back to the work of Wheeler on polyelectrons in 1946 [1]. Another and, perhaps, easier to imagine realization of the positron-electron interaction comes in the form of a positron attaching itself to an atom and forming an electronically stable bound state. Despite the simplicity of such systems, it took half a century for the theoretical predictions to provide a rigorous proof that a positron can bind to a neutral atom. The ambiguity was finally settled when two independent variational calculations were performed and demonstrated the electronic stability of the ground state of positronic lithium [2,3]. By now, a number of theoretical studies established that positron binding by electrically neutral atoms should be a common phenomenon. Around a dozen atoms are believed to be capable of binding a positron [4–19]. Yet, there has been no experimental evidence that demonstrates the existence of simple positronic atoms. All small bound positronic systems that have been observed so far either consist of light particles only (Ps$^-$, Ps$_2$) [20–24] or exhibit the chemical characteristics of positronium

compounds (PsH) [25]. Experimental measurements of the positron affinities with molecules are performed using the shifts of vibrational Feshbach resonances (VFRs) [8,26–28]. In the case of positronic atoms there have been some proposals for experimental detection using the shifts of VFRs [7,8], laser-assisted photorecombinations [29], or doing it on the basis of reactions with negative ions [30].

In this article, we study positronic beryllium, e^+[Be], a system in which a positron is attached to the beryllium atom. Its existence was first predicted in 1998 based on variational calculations that employed explicitly correlated Gaussians (ECGs) [5]. Successive theoretical works have confirmed the existence and enhanced the precision of that first conclusive calculation [6,12,14,31,32]. Furthermore, extrapolating configuration-interaction (CI) energies of the excited triplet P state to an infinite basis set limit hinted at possible positron binding in that state [33]. These predictions were later rigorously confirmed in accurate ECG calculations [12]. More recently, Strasburger carried out variational calculations employing ECG functions that showed the dynamic stability of excited triplet S state of positronic beryllium [14]. These calculations demonstrate that positron binding in excited states may be a rather common phenomenon, despite the fact that most literature studies so far have dealt with the ground states of positronic atoms.

The positron binding in both ground and excited states of atoms, even if it does take place, tends to be rather weak. For example, for the ground state of positronic lithium it amounts to just 0.0025 hartree (or 0.068 eV) [34]. For larger atoms that support positron attachment the magnitude of the binding energy may increase a little, yet it still remains small. For example, for the ground state of copper it is estimated at 0.0048–0.0062 hartree (0.13–0.17 eV) [13,16,35]. Not only does weak binding and cluster-like or halo-like structure [36]

*dm.tumakov@gmail.com
†pavel.rzhevskii@nu.edu.kz
‡toreniyaz.shomenov@nu.edu.kz
§sergiy.bubin@nu.edu.kz

042826-1

of positronic atoms pose challenges for reliable and accurate determination of the binding energy using traditional electronic structure methods but it also naturally raises a question of how significant the relativistic effects in such systems could be. Specifically, one may ask a question of whether the inclusion of relativistic corrections can alter the dynamic stability of a weakly bound positron–atom complex. Next, even if the conclusion about the stability remains unchanged, it is important to understand how sensitive the binding energy may be to the shifts and splittings of the energy levels caused by various relativistic effects as it may be helpful for guiding experimental measurements. Up to this date, there has been only a single study where this was investigated more or less systematically for two alkali-metal atoms (Li and Na) using an approach that is based on a model potential for a valence electron [37].

Building upon our earlier work concerning positronic beryllium [12], in this article we studied three states of this simple positron-atom complex: the ground singlet S state as well as the excited triplet S and P states (the multiplicity here refers to the subsystem of electrons). The ^3P state is particularly interesting since it gives nonzero fine-structure correction. Moreover, the spin-orbit correction in this state is not canceled out at all when the binding energy is determined, as is largely the case for other relativistic corrections, because the dissociation threshold corresponds to two subsystems (Ps and Be$^+$) in S states. For all systems and states considered in this work we adopted variational expansions of the wave functions in terms of thousands of thoroughly optimized all-particle explicitly correlated Gaussians. It allowed us to obtain highly accurate solutions to the few-particle nonrelativistic Schrödinger equation and then use them in the framework of the Breit–Pauli perturbation theory to study the significance of the relativistic effects. It should be noted that the wave functions we used not only accurately describe all electron-electron and electron-positron correlations, but they also account for small isotopic effects as the nonrelativistic Hamiltonian we employed includes nuclear degrees of freedom in the same way as those for the electrons and positron. As a result, we could reliably determine all necessary quantities at the nonrelativistic level of theory without resorting to any approximations.

II. THEORETICAL AND COMPUTATIONAL METHODS

A. Nonrelativistic Hamiltonian

In this work we deal with several few-particle systems comprised of particles that have different charges and masses. We begin with the full nonrelativistic Hamiltonian for an arbitrary system of N particles interacting via the Coulomb forces. Let m_i and q_i be their masses and charges respectively, while r_i are the Cartesian position vectors $(i = 1, \ldots, N)$ in the laboratory reference frame. In atomic units the Hamiltonian of such system is then given by

$$\mathcal{H}_{\text{NR}}^{\text{lab}} = -\sum_{i=1}^{N} \frac{1}{2m_i} \nabla_{r_i}^2 + \sum_{i=1}^{N} \sum_{j>i}^{N} \frac{q_i q_j}{r_{ij}}, \quad (1)$$

where ∇_{r_i} is the gradient with respect to the position of the ith particle and $r_{ij} = |r_i - r_j|$ is the distance between particles

i and j. If none of the particles are frozen in space (which happens when some particles have infinitely heavy masses) the above nonrelativistic Hamiltonian does not have discrete spectrum. The bound states are embedded into a continuum because the system as a whole may have a nonzero linear momentum. Thus, at the very first step, we must separate out the free motion of the center of mass. This can be achieved by a transformation from the $3N$ laboratory frame coordinates $\mathbf{r}_i$ to a set of new coordinates composed of three Cartesian coordinates of the center of mass and some $3N - 3$ internal coordinates. The choice of the internal coordinates is not unique. When we deal with systems containing a single heavy particle (e.g., atomic nucleus), which we may call particle 1 or the reference particle, it is natural to choose a set of internal coordinates comprised of relative positions of all other particles with respect to that reference particle, i.e.,

$$r_i = \mathbf{r}_{i+1} - \mathbf{r}_1 \ (i = 1, \ldots, n), \quad r_N = \mathbf{r}_{\text{cm}} = \sum_{i=1}^{N} \frac{m_i \mathbf{r}_i}{m_{\text{tot}}}. \quad (2)$$

Here we defined $n = N - 1$ and $m_{\text{tot}} = \sum_{i=1}^{N} m_i$ is the total mass of the system. With the above coordinate transformation the laboratory frame Hamiltonian (1) separates into the term that describes the motion of the center of mass, $\mathcal{H}_{\text{NR}}^{\text{cm}}$, and the one that describes the internal motion of the particles within the system:

$$\mathcal{H}_{\text{NR}}^{\text{lab}} = \mathcal{H}_{\text{NR}}^{\text{cm}} + \mathcal{H}_{\text{NR}}^{\text{int}}, \quad \mathcal{H}_{\text{NR}}^{\text{cm}} = -\frac{1}{2m_{\text{tot}}} \nabla_{r_N}^2, \quad (3)$$

$$\mathcal{H}_{\text{NR}}^{\text{int}} = -\nabla_r' M \nabla_r + \sum_{i=1}^{n} \frac{q_0 q_i}{r_i} + \sum_{i=1}^{n} \sum_{j<i}^{n} \frac{q_i q_j}{r_{ij}}. \quad (4)$$

Here for convenience we introduced the following notations:

$$r = \begin{pmatrix} r_1 \\ r_2 \\ \vdots \\ r_n \end{pmatrix}, \quad \nabla_r = \begin{pmatrix} \nabla_{r_1} \\ \nabla_{r_2} \\ \vdots \\ \nabla_{r_n} \end{pmatrix}, \quad (5)$$

$m_i = m_{i+1} \ (i = 0, \ldots, n)$, $q_i = q_{i+1} \ (i = 0, \ldots, n)$, $M = M \otimes \mathbf{I}$ is the Kronecker product of an $n \times n$ matrix M and a 3×3 identity matrix $\mathbf{I}$. Matrix M has diagonal elements $1/(2\mu_i)$ with $\mu_i = m_0 m_i/(m_0 + m_i)$, while all off-diagonal elements are equal to $1/(2m_0)$. The prime symbol stands for the vector or matrix transpose. Note that in these notations m_0 and q_0 refer to the nuclear mass and charge respectively. For species containing ^{9}Be isotope we adopt the value $m_0 = 16424.20551681$. In the case of $^\infty$Be we set nuclear mass m_0 to infinity.

B. Basis functions for Rayleigh–Ritz method and solution to the nonrelativistic problem

For small systems composed of three to eight particles, a particularly efficient approach to solve the nonrelativistic Schrödinger equation with Hamiltonian (4) is based on the variational method augmented with the use of explicitly correlated Gaussian (ECG) functions [38–45]. The ECG basis sets, which were initially introduced by Boys [38] and Singer [39] back in the 1960s, offer remarkable flexibility and efficiency

in a wide range of applications related to quantum few-body systems.

In the context of this work, we consider two cases: when the total orbital angular momentum L of the system is either 0 or 1 (S and P states, respectively). The spatial part of the corresponding ECGs can be written in a compact matrix form [46,47] as follows:

$$\phi_k^{(L=0,M_L=0)} = \exp[-\mathbf{r}'(A_k \otimes \mathbf{I})\mathbf{r}], \tag{6}$$

$$\phi_k^{(L=1,M_L=0)} = z_{i_k} \exp[-\mathbf{r}'(A_k \otimes \mathbf{I})\mathbf{r}], \tag{7}$$

where A_k is an $n \times n$ real symmetric matrix of nonlinear variational parameters (unique for each basis function ϕ_k). The basis in equation (7) that is suitable for systems with the total orbital angular momentum $L = 1$, contains a prefactor z_{i_k} which may be viewed as a Cartesian form of the angular function $r_{i_k} Y_{10}(\mathbf{r}_{i_k})$. Index i_k is an adjustable integer variational parameter that can vary between 1 and n. We note that it is also possible to use prefactors in the form $(x_{i_k} \pm iy_{i_k})/\sqrt{2}$ that correspond to the $M_L = \pm 1$ projection of the orbital angular momentum on the z axis. Basis functions (6) and (7) must be square integrable to be used in the expansions of wave functions that correspond to bound states. This requires positive definiteness of matrix A_k. The positive definiteness can be easily ensured if A_k is represented in the Cholesky-factored form, $A_k = L_k L_k'$, where L_k is a lower triangular matrix whose elements can be varied without any constrains.

To obtain accurate solutions to the nonrelativistic Schrödinger equation for positronic complexes and their parent ions we use the Rayleigh–Ritz method. In this process we adopt the spin-free formalism [48,49] with suitable permutational symmetry projector $\mathcal{Y}^r$. Many-particle wave function was expanded in terms of the properly symmetrized basis functions (6) or (7):

$$\psi(\mathbf{r}) = \sum_{k=1}^{\mathcal{K}} c_k \mathcal{Y}^r \phi_k(\mathbf{r}), \tag{8}$$

with the nonlinear parameters generated based on the same basis building and optimization strategy that was adopted in our previous works [50–53]. At each step of the nonlinear optimization process that aims to tune parameters A_k with the aim of minimizing the expectation value of nonrelativistic Hamiltonian (4), a generalized symmetric eigenvalue problem is solved to determine the expansion coefficients c_k:

$$\mathtt{H}c = \epsilon \mathtt{S}c, \tag{9}$$

where $\mathtt{H}$ and $\mathtt{S}$ are $\mathcal{K} \times \mathcal{K}$ Hamiltonian and overlap matrices, respectively, with the elements

$$\mathtt{H}_{kl} = \langle \mathcal{Y}^r \phi_k | \mathcal{H}_{\mathrm{NR}}^{\mathrm{int}} | \mathcal{Y}^r \phi_l \rangle = \langle \phi_k | \mathcal{H}_{\mathrm{NR}}^{\mathrm{int}} | (\mathcal{Y}^r)^\dagger \mathcal{Y}^r \phi_l \rangle,$$

$$\mathtt{S}_{kl} = \langle \mathcal{Y}^r \phi_k | \mathcal{Y}^r \phi_l \rangle = \langle \phi_k | (\mathcal{Y}^r)^\dagger \mathcal{Y}^r \phi_l \rangle,$$

c is a $\mathcal{K}$-component vector of the linear expansion coefficients, and ϵ is the eigenvalue corresponding to a specific ground or excited state that is being targeted. The dagger symbol stands for the adjoint operator.

The choice of the Young projection operator $\mathcal{Y}^r$ is not unique. Specifically, in the case of a singlet state of positronic beryllium (assuming that the nucleus is particle 1, positron is

particle 2, and electrons are particles 3–6) it can be chosen in the form

$$\mathcal{Y}^r = (\mathcal{I} + \mathcal{P}_{56}^r)(\mathcal{I} + \mathcal{P}_{34}^r)(\mathcal{I} - \mathcal{P}_{46}^r)(\mathcal{I} - \mathcal{P}_{35}^r),$$

where $\mathcal{I}$ is the identity operator, $\mathcal{P}_{ij}^r$ is the permutation of the spatial coordinate of the ith and jth particles, and to be concise we dropped the normalization factor. For a triplet state of positronic beryllium the projector can be chosen as

$$\mathcal{Y}^r = (\mathcal{I} + \mathcal{P}_{34}^r)(\mathcal{I} - \mathcal{P}_{36}^r - \mathcal{P}_{56}^r)(\mathcal{I} - \mathcal{P}_{35}^r).$$

C. Leading relativistic corrections

Even with a high quality and well-optimized wave function, the knowledge of nonrelativistic energy alone is often insufficient for making highly accurate calculations of the total and transition energies of the quantum states of atoms. To achieve high accuracy, it is necessary to consider relativistic and quantum electrodynamics (QED) effects in the calculations. The commonly employed and most practical approach for including these effects in the case of few-electron systems is to expand the total energy in terms of the fine-structure constant α [54,55]:

$$E_{\mathrm{TOT}} = E_{\mathrm{NR}} + \alpha^2 E_{\mathrm{REL}}^{(2)} + \alpha^3 E_{\mathrm{QED}}^{(3)} + \alpha^4 E_{\mathrm{HQED}}^{(4)} + \cdots. \tag{10}$$

Here E_{NR} is the nonrelativistic energy of the state under consideration, $\alpha^2 E_{\mathrm{REL}}^{(2)}$ is the leading relativistic corrections, $\alpha^3 E_{\mathrm{QED}}^{(3)}$ is the leading QED correction, and $\alpha^4 E_{\mathrm{HQED}}^{(4)}$ is the next-order QED correction. In the present work, we consider only the leading relativistic corrections that are proportional to α^2. The evaluation of each of the terms in (10) involves determining the expectation value of an effective operator, which represents the term being calculated. For instance, $E_{\mathrm{REL}}^{(2)}$ is computed as the expectation value of the Dirac–Breit Hamiltonian ($\mathcal{H}_{\mathrm{REL}}$) in the Pauli approximation [56,57] and contains the following contributions:

$$\mathcal{H}_{\mathrm{REL}} = \mathcal{H}_{\mathrm{MV}} + \mathcal{H}_{\mathrm{D}} + \mathcal{H}_{\mathrm{OO}} + \mathcal{H}_{\mathrm{SS}} + \mathcal{H}_{\mathrm{SO}} + \mathcal{H}_{\mathrm{A}}. \tag{11}$$

Here $\mathcal{H}_{\mathrm{MV}}, \mathcal{H}_{\mathrm{D}}, \mathcal{H}_{\mathrm{OO}}, \mathcal{H}_{\mathrm{SS}}, \mathcal{H}_{\mathrm{SO}}$, and $\mathcal{H}_{\mathrm{A}}$ are operators that are traditionally given the names of the mass–velocity, Darwin, orbit–orbit, spin–spin, spin–orbit, and annihilation channel interaction, respectively. The explicit forms of these operators in internal coordinates are as follows:

$$\mathcal{H}_{\mathrm{MV}} = -\frac{1}{8}\left[\frac{1}{m_0^3}\left(\sum_{i=1}^{n} \boldsymbol{\nabla}_{\mathbf{r}_i}\right)^4 + \sum_{i=1}^{n} \frac{1}{m_i^3} \boldsymbol{\nabla}_{\mathbf{r}_i}^4\right], \tag{12}$$

$$\mathcal{H}_{\mathrm{D}} = -\frac{\pi}{2}\left[\sum_{i=1}^{n} \frac{q_0 q_i}{m_i^2} \delta(\mathbf{r}_i) + \sum_{j=1}^{n} \sum_{i \neq j}^{n} \frac{q_i q_j}{m_i^2} \delta(\mathbf{r}_{ij})\right], \tag{13}$$

$$\mathcal{H}_{\mathrm{OO}} = -\frac{1}{2}\sum_{i=1}^{n}\sum_{j=1}^{n} \frac{q_0 q_j}{m_0 m_j}\left[\frac{1}{r_j}\boldsymbol{\nabla}'_{\mathbf{r}_i}\boldsymbol{\nabla}_{\mathbf{r}_j} + \frac{1}{r_j^3}\mathbf{r}'_j(\mathbf{r}'_j\boldsymbol{\nabla}_{\mathbf{r}_i})\boldsymbol{\nabla}_{\mathbf{r}_j}\right]$$

$$+ \frac{1}{2}\sum_{i=1}^{n}\sum_{j>i}^{n} \frac{q_i q_j}{m_i m_j}\left[\frac{1}{r_{ij}}\boldsymbol{\nabla}'_{\mathbf{r}_i}\boldsymbol{\nabla}_{\mathbf{r}_j} + \frac{1}{r_{ij}^3}\mathbf{r}'_{ij}(\mathbf{r}'_{ij}\boldsymbol{\nabla}_{\mathbf{r}_i})\boldsymbol{\nabla}_{\mathbf{r}_j}\right], \tag{14}$$

$$\mathcal{H}_{\mathrm{SS}} = \mathcal{H}_{\mathrm{SSF}} + \mathcal{H}_{\mathrm{SSN}}, \tag{15}$$

$$\mathcal{H}_{\text{SSF}} = -\frac{8\pi}{3}\sum_{i=1}^{n}\sum_{j>i}^{n}\frac{q_i q_j}{m_i m_j}s_i' s_j \delta(r_{ij}), \tag{16}$$

$$\mathcal{H}_{\text{SSN}} = \sum_{i=1}^{n}\sum_{j>i}^{n}\frac{q_i q_j}{m_i m_j}\left[\frac{(s_i' s_j)}{r_{ij}^3} - 3\frac{(s_i' r_{ij})(s_j' r_{ij})}{r_{ij}^5}\right], \tag{17}$$

$$\mathcal{H}_{\text{SO}} = \mathcal{H}_{\text{SO1}} + \mathcal{H}_{\text{SO2}}, \tag{18}$$

$$\mathcal{H}_{\text{SO1}} = -\sum_{i=1}^{n}\frac{q_0 q_i}{2m_i}\left(\frac{1}{m_i} + \frac{2}{m_0}\right)\frac{s_i'}{r_i^3}[r_i \times p_i], \tag{19}$$

$$\mathcal{H}_{\text{SO2}} = -\sum_{i=1}^{n}\sum_{\substack{j=1 \\ j\neq i}}^{n}\left\{\frac{q_0 q_i}{m_0 m_i}\frac{s_i'}{r_i^3}[r_i \times p_j]\right.$$
$$\left. + \frac{q_i q_j}{2m_i}\frac{s_i'}{r_{ij}^3}\left[(r_i - r_j) \times \left(\frac{1}{m_i}p_i - \frac{2}{m_j}p_j\right)\right]\right\}, \tag{20}$$

$$\mathcal{H}_{\text{A}} = -2\pi\sum_{\substack{i=1 \\ \text{over } e^+e^- \text{ pairs only}}}^{n}\sum_{j=1, j\neq i}^{n}\frac{q_i q_j}{m_i m_j}\left(\frac{3}{4} + s_i' s_j\right)\delta(r_{ij}). \tag{21}$$

The above expressions are written with the assumption that the first particle in the system is the nucleus, while the numbers of electrons and positrons are arbitrary. s_i ($i = 0, \ldots, n$) stands for the spin operator of particle $i + 1$. In formula (15) the spin–spin interaction is split into a sum of the Fermi contact term, $\mathcal{H}_{\text{SSF}}$, and the noncontact (often called dipolar) term, $\mathcal{H}_{\text{SSN}}$. The noncontact part corresponds to a classical expression for the interaction of two magnetic dipoles and contributes to a fine-structure splitting of energy levels. The Fermi contact term $\mathcal{H}_{\text{SSF}}$ shifts the energy levels without splitting them. Operators $\mathcal{H}_{\text{SO1}}$ and $\mathcal{H}_{\text{SO2}}$ in the literature are often referred to as "spin-same-orbit" and "spin-other-orbit" interactions, respectively.

It should be noted that the contribution due to the spin-orbit term, $\mathcal{H}_{\text{SO}}$, vanishes for S states. Also, the expectation value of the noncontact part of the spin–spin term, $\mathcal{H}_{\text{SSN}}$, vanishes for all S states and doublet non-S states. The annihilation channel interaction, $\mathcal{H}_{\text{A}}$, is only present for systems containing positrons as the summation goes over electron-positron pairs. Lastly, we note that in our treatment we do not include the spin–spin interactions that involve nuclear spin and which give rise to what is known as the hyperfine structure. While they are formally proportional to α^2, they are greatly suppressed by the large value of the nuclear mass and can be safely neglected in our analysis that aims to account for the most significant relativistic effects only.

All terms in $\mathcal{H}_{\text{REL}}$, except for $\mathcal{H}_{\text{OO}}$, $\mathcal{H}_{\text{SO}}$, and $\mathcal{H}_{\text{SSN}}$, contain singular operators, namely, one- and two-particle Dirac δ functions, $\delta(r_i)$ and $\delta(r_{ij})$ [in three dimensions, the δ function is defined as $\delta(r_i) \equiv \delta(x_i)\delta(y_i)\delta(z_i)$], and the fourth power of the nabla operator, $\nabla_{r_i}^4$. When one computes their expectation values with a variational wave function, it results in a notably slower convergence as the basis size is increased. Such behavior takes place because the sampling of the wave function is essentially restricted locally (within a small region of singularity, e.g., when $r_i = 0$), amplifying any local inaccuracies of the wave function. This sharply contrasts with situations involving "well-behaved" operators, where the in-

tegrand contains no singularities and local inaccuracies of the approximate wave function largely cancel out globally. Some effective strategies have been developed to remedy this problem in the calculations of few-electron systems [58–63]. In the present work we employ the regularization approach commonly referred to as drachmanization [61,62] to compute the expectation values of $\mathcal{H}_{\text{MV}}$, $\mathcal{H}_{\text{D}}$, $\mathcal{H}_{\text{SSF}}$, and $\mathcal{H}_{\text{A}}$. A number of our previous calculations on small atoms and ions have demonstrated that it notably improves the convergence of the results [51–53,64,65]. To indicate that a specific expectation value was regularized, we use the tilde symbol, e.g., $\langle\tilde{\mathcal{H}}_{\text{MV}}\rangle$ or $\langle\tilde{\delta}(r_1)\rangle$.

D. Expectation values of spin-dependent operators and the framework of spin-free formalism

In calculations of the nonrelativistic energy and the mean values of the spin-independent operators we adopt the spin-free formalism, which involves the spatial wave function only. In this formalism, a suitable permutational symmetry projector is applied to each basis function, as shown in (8). To construct a suitable symmetry projector, we follow the standard procedure involving Young operators [48,49]. However, in order to compute the expectation values of the operators that are explicitly spin-dependent, one must use the total (spatial + spin) wave function, which can be represented as

$$\Psi(r, \sigma) = \mathcal{A}[\Theta(\sigma)\psi(r)], \tag{22}$$

where $\Theta(\sigma)$ is a spin function, σ is an n-component vector constructed from spin coordinates σ_i ($i = 1, \ldots, n$) and the antisymmetrizer $\mathcal{A}$ is defined as

$$\mathcal{A} = \frac{1}{\sqrt{n_e!}}\sum_{i}\varepsilon(\mathcal{P}_i)\mathcal{P}_i. \tag{23}$$

Here index i runs over the electrons' symmetric group that has $n_e!$ elements, n_e is the number of electrons in the system, $\mathcal{P}_i$ is the permutation operator acting on both spin and spatial variables, and $\varepsilon(\mathcal{P}_i)$ is the parity of the permutation. For any operator $\mathcal{O}$, which can be factorized as a product of the spatial and spin operators $\mathcal{O}^r \mathcal{O}^\sigma$ and commutes with any electronic permutation $\mathcal{P}_i$, we can calculate the mean value as

$$\langle\mathcal{O}\rangle = \sum_{i}\varepsilon(\mathcal{P}_i)\langle\Theta|\mathcal{O}^\sigma \mathcal{P}_i^\sigma|\Theta\rangle_\sigma \langle\psi|\mathcal{O}^r \mathcal{P}_i^r|\psi\rangle_r, \tag{24}$$

where $\langle\ldots\rangle_\sigma$ and $\langle\ldots\rangle_r$ stand for averaging over spin and spatial coordinates, respectively. Let S_e and S_e be the operator of the total spin and the corresponding quantum number for the subsystem composed of all electrons, while S and S are the total spin operator and the corresponding quantum number for all light particles in the system (positron and electrons). Both S_e and S are good quantum numbers in the nonrelativistic theory. For convenience, let us assume definite projections of the total spin and the total orbital angular momentum on the z axis, i.e., $M_S = S$, $M_L = L$ [note that the prefactor in Eq. (7) will change from z_{i_k} to $(x_{i_k} + iy_{i_k})/\sqrt{2}$]. To construct the *electronic* spin function θ_{S_e, S_e} (here the first subscript denotes the spin and the second one denotes its z projection) one should build the spin Young operator $\mathcal{Y}^\sigma$ corresponding to the transposed spatial Young tableau, which was used in

TABLE I. Convergence of total nonrelativistic energies and positron binding energies ϵ_{NR} (all values are in atomic units) with the number of ECG basis functions, $\mathcal{K}$. The entries marked with "∞" correspond to the extrapolated values. For comparison we also show values obtained in previous best calculations in Refs. [12] and [14].

$\mathcal{K}$	Ref.	Energy		ϵ_{NR} ($\times 10^3$)
		${}^9\mathrm{Be}(^1S)$	$e^+[{}^9\mathrm{Be}](^{2;1}S)$	
500		−14.666 428 418	−14.669 153	2.725
1000		−14.666 434 601	−14.669 554	3.119
2000		−14.666 435 372	−14.669 662	3.227
3000		−14.666 435 492	−14.669 681	3.245
4000		−14.666 435 516	−14.669 687	3.251
5000		−14.666 435 522	−14.669 690	3.254
6000		−14.666 435 524	−14.669 691	3.255
∞		−14.666 435 525(1)	−14.669 692(1)	3.256(1)
		${}^\infty\mathrm{Be}(^1S)$	$e^+[{}^\infty\mathrm{Be}](^{2;1}S)$	
6000		−14.667 356 506	−14.670 609	3.253
∞		−14.667 356 507(1)	−14.670 610(1)	3.254(1)
2500	[12]	−14.667 356 45	−14.670 593	3.236
5962	[14]		−14.670 60787	3.251
∞	[14]		−14.670 611(3)	3.254
		${}^9\mathrm{Be}^+(^2S)$	$e^+[{}^9\mathrm{Be}](^{2,4;3}S)$	
500		−14.323 863 152 43	−14.575 998	2.135
1000		−14.323 863 470 38	−14.576 702	2.838
2000		−14.323 863 493 01	−14.576 915	3.052
3000		−14.323 863 494 48	−14.576 968	3.104
4000		−14.323 863 494 75	−14.576 985	3.121
5000		−14.323 863 494 79	−14.576 992	3.129
6000		−14.323 863 494 82	−14.576 996	3.132
∞		−14.323 863 494 85(3)	−14.577 000(4)	3.137(5)
		${}^\infty\mathrm{Be}^+(^2S)$	$e^+[{}^\infty\mathrm{Be}](^{2,4;3}S)$	
6000		−14.324 763 176 78	−14.577 897	3.134
∞		−14.324 763 176 81(3)	−14.577 901(4)	3.138(5)
6524	[14]		−14.577 89878	3.136
∞	[14]		−14.577 902(3)	3.139
		${}^9\mathrm{Be}^+(^2S)$	$e^+[{}^9\mathrm{Be}](^{2,4;3}P)$	
500		−14.323 863 152 43	−14.572 775	−1.089
1000		−14.323 863 470 38	−14.574 263	0.400
2000		−14.323 863 493 01	−14.574 785	0.921
3000		−14.323 863 494 48	−14.574 909	1.045
4000		−14.323 863 494 75	−14.574 953	1.089
5000		−14.323 863 494 79	−14.574 975	1.111
6000		−14.323 863 494 82	−14.574 985	1.121
∞		−14.323 863 494 85(3)	−14.574 994(9)	1.130(9)
		${}^\infty\mathrm{Be}^+(^2S)$	$e^+[{}^\infty\mathrm{Be}](^{2,4;3}P)$	
6000		−14.324 763 176 78	−14.575 886	1.123
∞		−14.324 763 176 81(3)	−14.575 895(9)	1.132(9)
2500	[12]	−14.324 763 18	−14.575 765	1.002

the spin-free calculations. Then

$$\theta_{S_e,S_e} = \mathcal{Y}^\sigma \theta, \tag{25}$$

where θ is a primitive n_e-electron spin function such that

$$\boldsymbol{S}_{e,z}\theta = S_e\theta, \tag{26}$$

$$\mathcal{Y}^\sigma\theta \neq 0. \tag{27}$$

If the system under consideration only contains electrons, then $\Theta = \theta_{S_e,S_e}$, and one can calculate the mean values using Eq. (24).

TABLE II. Mean interparticle distances (in a.u.) calculated for the positronic systems and parent atomic or ionic states and extrapolated to the infinite basis set.

State	$\langle r_{ne^-}\rangle$	$\langle r_{ne^+}\rangle$	$\langle r_{e^-e^-}\rangle$	$\langle r_{e^-e^+}\rangle$
${}^9\mathrm{Be}(^1S)$	1.493194(0)		2.545442(0)	
$e^+[{}^9\mathrm{Be}](^{2;1}S)$	1.535790(3)	10.0223(5)	2.606376(6)	9.9799(5)
${}^9\mathrm{Be}^+(^2S)$	1.033863(0)		1.755787(0)	
$e^+[{}^9\mathrm{Be}](^{2,4;3}S)$	2.7603(3)	10.054(2)	4.9720(6)	8.822(2)
$e^+[{}^9\mathrm{Be}](^{2,4;3}P)$	2.366(3)	9.729(10)	4.227(5)	8.918(8)

For positron-atom complexes we should build two spin functions Θ_{high} and Θ_{low} corresponding to the value of the total spin quantum number $S = S_e \pm 1/2$ (if $S_e = 0$ then $\Theta_{low} = \Theta_{high}$). If we adopt a notation where in the product of spin functions we first write the positron spin function and second the spin function of the electrons, then according to the rules of addition of angular momenta:

$$\Theta_{high} = \alpha\,\theta_{S_e,S_e}, \tag{28}$$

$$\Theta_{low} = C^{S_e-\frac{1}{2},S_e-\frac{1}{2}}_{\frac{1}{2},-\frac{1}{2},S_e,S_e}\beta\,\theta_{S_e,S_e} + C^{S_e-\frac{1}{2},S_e-\frac{1}{2}}_{\frac{1}{2},\frac{1}{2},S_e,S_e-1}\alpha\,\theta_{S_e,S_e-1}, \tag{29}$$

where $C^{S,M}_{S_1,M_1,S_2,M_2}$ are the Clebsch–Gordan coefficients, and α and β are the eigenstates of positronic spin projector $s_{p,z}$ with the eigenvalues of $1/2$ and $-1/2$, respectively. Spin functions for the right-hand side can be generated with the electronic and positronic lowering operators $\boldsymbol{S}_{e,-}$ and $\boldsymbol{s}_{p,-}$:

$$\alpha\theta_{S_e,S_e-1} \sim \boldsymbol{S}_{e,-}\Theta_{high}, \quad \beta\theta_{S_e,S_e} \sim \boldsymbol{s}_{p,-}\Theta_{high}. \tag{30}$$

The spin-orbit and noncontact spin–spin operators can be expressed as a sum of scalar products of spin and spatial tensor operators of rank k ($k = 1$ for $\mathcal{H}_{SO}$ and $k = 2$ for $\mathcal{H}_{SSN}$). For the principal case ($S = M_S$, $L = M_L$) the mean value of such operator $\mathcal{O} = \sum_j T^{(k)}_j \cdot U^{(k)}_j$ when sandwiched between the states with the same value of S and L can be calculated as follows [66,67]:

$$\langle\mathcal{O}\rangle_J = C_J \sum_i \varepsilon(\mathcal{P}_i) \sum_{\{j\}} \langle\Theta_{SS}|T^{(k)}_{j,0}\mathcal{P}^\sigma_i|\Theta_{SS}\rangle_\sigma$$

$$\times \langle\psi_{LL,\gamma}|U^{(k)}_{j,0}\mathcal{P}^r_i|\psi_{LL,\gamma}\rangle_r, \tag{31}$$

where i runs over all electron permutations and $\{j\}$ denotes the sum over all particles. The first two subscripts in the spatial part of the wave function denote the total orbital momentum and its projection, while the subscript γ refer to all the other quantum numbers that uniquely identify the state. The second subscript in tensor operators denotes a component. Angular coefficient C_J reflects rotational properties of the matrix element and is expressed through the $6j$ symbol:

$$C_J = \delta_{JJ'}\delta_{M_J M_{J'}}(-1)^{S+L+J}$$

$$\times \frac{\sqrt{(2S-k)!\,(2S+k+1)!\,(2L-k)!\,(2L+k+1)!}}{(2S)!\,(2L)!}$$

$$\times \begin{Bmatrix} S & S & k \\ L & L & J \end{Bmatrix}, \tag{32}$$

where J is the total angular momentum of the system and M_J is its projection.

TABLE III. Convergence of the spin-independent relativistic corrections and two-particle (nucleus–electron, electron–electron, and electron–positron) contact densities with the number of basis functions $\mathcal{K}$ for different systems and isotopes. All values are in a.u.

$\mathcal{K}$	$\langle \tilde{\delta}_{\mathrm{n}e^-} \rangle$	$\langle \tilde{\delta}_{e^-e^-} \rangle$	$\langle \tilde{\delta}_{e^-e^+} \rangle$	$\langle \tilde{\mathcal{H}}_{\mathrm{MV}} \rangle$	$\langle \tilde{\mathcal{H}}_{\mathrm{D}} \rangle$	$\langle \mathcal{H}_{\mathrm{OO}} \rangle$
			$^9\mathrm{Be}(^1S)$			
500	8.840 587 591	0.267 501 933		−270.640 669 4	217.145 907 6	−0.918 508 83
1000	8.840 613 913	0.267 505 901		−270.637 675 6	217.146 494 3	−0.918 464 34
2000	8.840 616 460	0.267 506 202		−270.637 204 0	217.146 552 7	−0.918 462 69
3000	8.840 617 149	0.267 506 263		−270.636 811 7	217.146 568 8	−0.918 461 73
4000	8.840 617 270	0.267 506 276		−270.636 754 4	217.146 571 6	−0.918 461 64
5000	8.840 617 325	0.267 506 281		−270.636 665 0	217.146 572 9	−0.918 461 60
6000	8.840 617 338	0.267 506 283		−270.636 661 1	217.146 573 2	−0.918 461 59
			$^\infty\mathrm{Be}(^1S)$			
6000	8.842 251 637	0.267 550 914		−270.703 631 1	217.186 806 3	−0.891 823 59
			$^9\mathrm{Be}^+(^2S)$			
500	11.699 524 125	0.526 758 279		−268.249 805 8	215.566 254 4	−0.936 298 89
1000	11.699 528 906	0.526 758 678		−268.249 355 7	215.566 340 8	−0.936 297 60
2000	11.699 529 294	0.526 758 732		−268.248 993 7	215.566 347 6	−0.936 297 17
3000	11.699 529 331	0.526 758 736		−268.248 964 5	215.566 348 3	−0.936 297 11
4000	11.699 529 340	0.526 758 737		−268.248 904 1	215.566 348 4	−0.936 297 09
5000	11.699 529 341	0.526 758 737		−268.248 899 4	215.566 348 4	−0.936 297 09
6000	11.699 529 342	0.526 758 737		−268.248 892 4	215.566 348 4	−0.936 297 08
			$^\infty\mathrm{Be}^+(^2S)$			
6000	11.701 685 284	0.526 846 196		−268.315 110 1	215.606 162 7	−0.909 902 36
			$e^+[^9\mathrm{Be}](^{2;1}S)$			
500	8.830 690 578	0.266 941 819	0.002 183 7	−270.309 429 7	216.935 242 1	−0.941 260 13
1000	8.831 748 483	0.266 991 092	0.002 150 4	−270.341 209 8	216.960 423 9	−0.940 943 22
2000	8.832 060 256	0.267 005 073	0.002 159 3	−270.346 755 8	216.968 086 8	−0.941 046 93
3000	8.832 109 692	0.267 008 877	0.002 161 2	−270.345 393 7	216.969 276 8	−0.941 063 19
4000	8.832 131 920	0.267 010 108	0.002 161 3	−270.344 855 5	216.969 812 0	−0.941 058 00
5000	8.832 139 174	0.267 010 606	0.002 161 4	−270.344 768 2	216.969 986 1	−0.941 059 59
6000	8.832 142 599	0.267 010 909	0.002 161 6	−270.344 536 6	216.970 068 1	−0.941 060 80
			$e^+[^\infty\mathrm{Be}](^{2;1}S)$			
6000	8.833 778 562	0.267 055 642	0.002 160 6	−270.411 544 1	217.010 329 1	−0.914 436 39
			$e^+[^9\mathrm{Be}](^{2,4;3}S)$			
500	8.758 346 623	0.262 732 519	0.007 367 0	−267.791 470 7	215.261 501 0	−0.982 003 70
1000	8.758 970 614	0.262 743 631	0.007 201 4	−267.821 883 9	215.274 856 2	−0.977 375 26
2000	8.759 228 282	0.262 758 289	0.007 148 9	−267.824 915 2	215.280 382 4	−0.975 781 25
3000	8.759 321 953	0.262 763 170	0.007 138 5	−267.826 343 5	215.282 511 0	−0.975 518 69
4000	8.759 360 015	0.262 765 208	0.007 135 7	−267.827 857 2	215.283 392 3	−0.975 466 57
5000	8.759 370 748	0.262 766 509	0.007 133 9	−267.826 669 4	215.283 614 4	−0.975 414 93
6000	8.759 379 186	0.262 767 063	0.007 132 9	−267.826 328 6	215.283 803 7	−0.975 391 77
			$e^+[^\infty\mathrm{Be}](^{2,4;3}S)$			
6000	8.760 991 466	0.262 810 592	0.007 132 2	−267.892 345 9	215.323 495 5	−0.949 032 96
			$e^+[^9\mathrm{Be}](^{2,4;3}P)$			
500	8.735 093 018	0.261 783 350	0.004 785 9	−267.030 973 2	214.662 670 8	−0.888 870 00
1000	8.739 453 551	0.261 945 499	0.005 016 0	−267.182 371 8	214.771 968 1	−0.895 948 61
2000	8.741 448 989	0.262 023 993	0.005 122 6	−267.245 925 7	214.821 928 9	−0.899 678 77
3000	8.741 897 830	0.262 043 357	0.005 140 0	−267.257 700 1	214.833 051 8	−0.900 304 16
4000	8.742 075 104	0.262 051 374	0.005 148 1	−267.262 950 8	214.837 453 8	−0.900 605 75
5000	8.742 170 147	0.262 055 615	0.005 152 4	−267.265 143 6	214.839 813 7	−0.900 758 07
6000	8.742 221 861	0.262 058 381	0.005 155 2	−267.266 423 8	214.841 095 3	−0.900 858 25
			$e^+[^\infty\mathrm{Be}](^{2,4;3}P)$			
6000	8.743 833 567	0.262 101 876	0.005 154 5	−267.332 369 2	214.880 772 7	−0.874 566 10

TABLE IV. Convergence of the expectation values of the Fermi contact spin–spin interaction, $\langle \mathcal{H}_{\mathrm{SSF}} \rangle$, for considered systems with the number of basis functions $\mathcal{K}$. All values are in a.u.

$\mathcal{K}$	Be(^1S)	Be$^+$(^2S)	e^+[Be]($^{2;1}S$)	e^+[Be]($^{2;3}S$)	e^+[Be]($^{4;3}S$)	e^+[Be]($^{2;3}P$)	e^+[Be]($^{4;3}P$)
				^{9}Be			
500	10.084 614 72	9.929 162 216	10.064 447	9.782 987	9.968 189 8	9.792 351	9.912 588
1000	10.084 739 71	9.929 167 445	10.065 647	9.785 309	9.966 302 2	9.792 624	9.918 541
2000	10.084 747 36	9.929 168 211	10.065 949	9.786 241	9.965 897 6	9.792 887	9.921 451
3000	10.084 748 94	9.929 168 258	10.066 039	9.786 459	9.965 852 4	9.793 086	9.922 080
4000	10.084 749 19	9.929 168 274	10.066 067	9.786 542	9.965 863 6	9.793 142	9.922 339
5000	10.084 749 31	9.929 168 277	10.066 077	9.786 592	9.965 868 1	9.793 169	9.922 472
6000	10.084 749 34	9.929 168 278	10.066 083	9.786 613	9.965 865 0	9.793 196	9.922 569
				$^\infty$Be			
6000	10.086 431 90	9.930 816 839	10.067 770	9.788 267	9.967 501 3	9.794 850	9.924 205

For the mean value of $\mathcal{H}_{\mathrm{SO}}$ we have

$$T_{j,0}^{(1)} = s_{j,z}, \tag{33}$$

$$U_{j,0}^{(1)} = i\frac{q_0 q_j}{2m_j}\left(\frac{1}{m_j} + \frac{2}{m_0}\right)\frac{1}{r_j^3}[\boldsymbol{r}_j \times \boldsymbol{\nabla}_{\boldsymbol{r}_j}]_z$$
$$+ i\sum_{\substack{k=1 \\ k \neq j}}^{n}\left\{\frac{q_0 q_j}{m_0 m_j}\frac{1}{r_j^3}[\boldsymbol{r}_j \times \boldsymbol{\nabla}_{\boldsymbol{r}_k}]_z \right.$$
$$\left. - \frac{q_j q_k}{2m_j}\frac{1}{r_{jk}^3}\left[\boldsymbol{r}_{jk} \times \left(\frac{2}{m_k}\boldsymbol{\nabla}_{\boldsymbol{r}_k} - \frac{1}{m_j}\boldsymbol{\nabla}_{\boldsymbol{r}_j}\right)\right]_z\right\}. \tag{34}$$

For the mean value of $\mathcal{H}_{\mathrm{SSN}}$,

$$T_{jk,0}^{(2)} = \frac{1}{\sqrt{6}}(3s_{j,z}s_{k,z} - \boldsymbol{s}_j'\boldsymbol{s}_k), \tag{35}$$

$$U_{jk,0}^{(2)} = \frac{1}{\sqrt{6}}\left[\left(3\left(\boldsymbol{\nabla}_{\boldsymbol{r}_j}\right)_z\left(\boldsymbol{\nabla}_{\boldsymbol{r}_k}\right)_z - \boldsymbol{\nabla}_{\boldsymbol{r}_j}'\boldsymbol{\nabla}_{\boldsymbol{r}_k}\right)\frac{1}{r_{jk}}\right], \tag{36}$$

where the gradients act only on $1/r_{jk}$.

For the e^+[Be($^{4;3}P$)] state $C_{J=\frac{1}{2},\frac{3}{2},\frac{5}{2}}^{\mathrm{SO}} = -5/3, -2/3, 1$, and $C_{J=\frac{1}{2},\frac{3}{2},\frac{5}{2}}^{\mathrm{SSN}} = 5, -4, 1$. For the e^+[Be($^{2;3}P$)] state $C_{J=\frac{1}{2},\frac{3}{2}}^{\mathrm{SO}} = -2$, 1 and noncontact spin–spin term vanishes.

It should be mentioned that our calculations do not include the off-diagonal matrix elements corresponding to states with different S and L quantum numbers. However, it is estimated

that their contribution is rather insignificant in ^3P states of Be [67].

III. RESULTS AND DISCUSSION

In what follows each term of a positron-atom complex is labeled as $^{2S+1;2S_e+1}L_J$ ($L = S, P$) in accordance with Ref. [68]. We omit the J value if it is not relevant.

A. Nonrelativistic energies and structural properties

First, we calculated nonrelativistic energies for the positronic complexes and their parent atoms or ions by minimizing the expectation value of nonrelativistic Hamiltonian (4). The results are presented in Table I for different basis sizes $\mathcal{K}$ to demonstrate the convergence of the energies. We compare our results corresponding to the infinite nuclear mass with those obtained in earlier works [12,14]. Note that the smaller basis sets (up to 2500 ECGs) for Be$^+$(^2S), Be(^1S), e^+[Be]($^{2;1}S$), and e^+[Be]($^{2,4;3}P$) in present calculations were adapted from Ref. [12]. Larger bases (3000 ECGs and up) were generated by adding new ECGs and re-optimizing the nonlinear parameters of the entire set of basis functions as described in Refs. [50–53].

The value of a positron binding energy ϵ_{NR} is calculated differently depending on the decay channel of the positronic

TABLE V. Convergence of the expectation values of the annihilation channel interaction, $\langle \mathcal{H}_{\mathrm{A}} \rangle$, with the number of basis functions $\mathcal{K}$. All values are in a.u.

$\mathcal{K}$	e^+[Be]($^{2;1}S$)	e^+[Be]($^{2;3}S$)	e^+[Be]($^{4;3}S$)	e^+[Be]($^{2;3}P$)	e^+[Be]($^{4;3}P$)
			^{9}Be		
500	0.041 162	0.046 263	0.185 165	0.030 094	0.120 271
1000	0.040 533	0.045 247	0.180 991	0.031 592	0.126 029
2000	0.040 702	0.044 925	0.179 667	0.032 277	0.128 700
3000	0.040 737	0.044 861	0.179 406	0.032 389	0.129 134
4000	0.040 739	0.044 844	0.179 335	0.032 442	0.129 339
5000	0.040 742	0.044 833	0.179 290	0.032 469	0.129 446
6000	0.040 744	0.044 827	0.179 265	0.032 487	0.129 517
			$^\infty$Be		
6000	0.040 726	0.044 822	0.179 248	0.032 482	0.129 498

TABLE VI. Convergence of the spin–orbit and noncontact spin–spin operators' mean values $\langle \mathcal{H}_{SO(SSN)} \rangle_J / C_J^{SO(SSN)}$ with the number of basis functions $\mathcal{K}$ for $e^+[^9\text{Be}](^{2,4;3}P)$. Labels "high" and "low" stand for the states $e^+[^9\text{Be}](^{4;3}P)$ and $e^+[^9\text{Be}](^{2;3}P)$, respectively. All values are in a.u.

$\mathcal{K}$	$\langle \mathcal{H}_{SO1} \rangle_{\text{high}}$	$\langle \mathcal{H}_{SO2} \rangle_{\text{high}}$	$\langle \mathcal{H}_{SO1} \rangle_{\text{low}}$	$\langle \mathcal{H}_{SO2} \rangle_{\text{low}}$	$\langle \mathcal{H}_{SSN} \rangle_{\text{high}}$
			^{9}Be		
500	0.155 00	−0.108 93	0.104 06	−0.073 36	0.001 32
1000	0.147 82	−0.103 05	0.099 29	−0.069 46	0.001 22
2000	0.144 05	−0.100 13	0.096 77	−0.067 51	0.001 17
3000	0.143 14	−0.099 39	0.096 16	−0.067 02	0.001 16
4000	0.142 76	−0.099 10	0.095 91	−0.066 83	0.001 15
5000	0.142 56	−0.098 94	0.095 77	−0.066 72	0.001 15
6000	0.142 45	−0.098 85	0.095 70	−0.066 66	0.001 15
			$^\infty$Be		
6000	0.142 45	−0.098 84	0.095 70	−0.066 66	0.001 15

complex:

$$\epsilon_{\text{NR}} = E_{\text{NR}}(\text{Be}) - E_{\text{NR}}(e^+[\text{Be}]) \quad (37)$$

for the $e^+[\text{Be}](^{2;1}S)$, and

$$\epsilon_{\text{NR}} = E_{\text{NR}}(\text{Be}^+) - 0.25 - E_{\text{NR}}(e^+[\text{Be}]) \quad (38)$$

for $e^+[\text{Be}](^{2,4;3}S)$ and $e^+[\text{Be}](^{2,4;3}P)$, where -0.25 is the binding energy of the positronium in its ground state.

The results of our nonrelativistic calculations for S states are in perfect agreement with the values obtained in Ref. [14] that adopted a similar computational approach and comparable basis size. As one can see the nonrelativistic value of
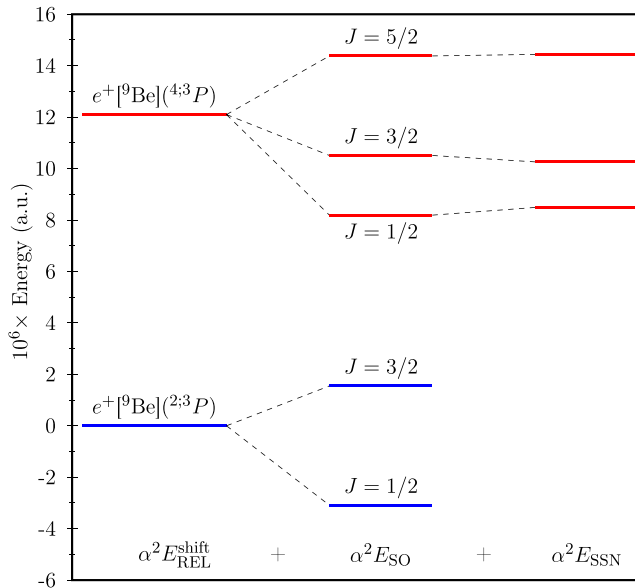

FIG. 1. Fine-structure splitting of the $e^+[^9\text{Be}](^{2;3}P)$ and $e^+[^9\text{Be}](^{4;3}P)$ states. $E_{\text{REL}}^{\text{shift}}$ corresponds to the total relativistic energy without the spin-orbit and noncontact spin–spin corrections. The vertical axis in this figure is shifted so that $E_{\text{REL}}^{\text{shift}}$ is zero for the doublet state. The difference in $E_{\text{REL}}^{\text{shift}}$ between the doublet and quartet states comes from the Fermi contact and annihilation channel interactions. The noncontact spin–spin term for the doublet state vanishes due to the rotational symmetry.

the positron binding energy for the P state differs from the value from Ref. [12] by about 12%, which is attributed to a significant increase of the basis size (6000 ECG basis functions in the present work vs 2500 functions in Ref. [12]) and more thorough optimization of the nonlinear parameters at later stages of the calculations.

We also note that the negative positron binding energy of $e^+\text{Be}(^{2,4;3}P)$ for $\mathcal{K} = 500$ is due to the fact that the convergence of the nonrelativistic energy for this state is slower. It takes quite a few ECGs and a lot of numerical effort to converge the total nonrelativistic energy within the tolerance that is comparable or smaller than the magnitude of the (tiny) positron affinity. Also, in general, obtaining the same level of accuracy for a system with a larger number of particles (e.g., six-particle $e^+[\text{Be}]$ vs four-particle Be^+) requires a considerably larger number of basis functions.

As the numbers in Table I show the finite value of the mass of the Be nucleus has vanishingly small effect on the positron binding energies, changing it in the third figure after the decimal point. The nuclear recoil effects in the positronic beryllium and its parent atom or ion largely cancel out.

Based on their structural properties, the positron–atom complexes can be schematically considered as mixtures of two major configurations: a positron "orbiting" slightly polarized atom and positronium atom interacting with the atomic ion. In Table II we show the mean interparticle distances for the positronic systems and parent atomic or ionic states. It can be seen that the value of $\langle r_{ne^-} \rangle$ is really close for $^9\text{Be}(^1S)$ and $e^+[^9\text{Be}](^{2;1}S)$, which suggests that the atom is only slightly polarized when a positron is attached. For the triplet states of the positron-atom complexes situation is opposite: both nucleus–electron $\langle r_{ne^-} \rangle$ and electron–electron $\langle r_{e^-e^-} \rangle$ mean distances are much larger when a positron is attached, which is consistent with the model of a positronium atom orbiting the parent ion. It should be noted that the mean electron-positron distance $\langle r_{e^-e^+} \rangle$ in all considered states of $e^+[\text{Be}]$, which ranges from 8.82 to 9.98 a.u., is much larger than it is in an isolated positronium atom, where it takes the value of 3 a.u. This is a reflection of extremely weak binding of the positron or positronium to the beryllium atom or ion, respectively. In other words, in all states of $e^+[\text{Be}]$ the positron is far from the inner electrons of beryllium.

TABLE VII. Convergence of total relativistic correction $\alpha^2 \langle \mathcal{H}_{\text{REL}} \rangle$ with the number of basis functions $\mathcal{K}$. All values are in $m$hartree.

$\mathcal{K}$	Be(^1S)	Be$^+$(^2S)	e^+[Be]($^{2;1}S$)	e^+[Be]($^{2;3}S$)	e^+[Be]($^{4;3}S$)
			^{9}Be		
500	−2.360 561 0	−2.326 588 3	−2.354 234	−2.326 164	−2.308 905
1000	−2.360 361 3	−2.326 559 4	−2.354 538	−2.326 757	−2.309 890
2000	−2.360 332 6	−2.326 539 7	−2.354 406	−2.326 506	−2.309 764
3000	−2.360 310 7	−2.326 538 1	−2.354 264	−2.326 447	−2.309 729
4000	−2.360 307 5	−2.326 534 9	−2.354 205	−2.326 474	−2.309 763
5000	−2.360 302 6	−2.326 534 6	−2.354 190	−2.326 394	−2.309 688
6000	−2.360 302 4	−2.326 534 3	−2.354 173	−2.326 364	−2.309 660
			$^\infty$Be		
6000	−2.360 218 1	−2.326 446 9	−2.354 091	−2.326 274	−2.309 572

B. Relativistic corrections

We present all data for the mean values that appear in individual terms of Eq. (11) in Tables III to VI.

In Table III one can see the convergence of the expectation values of two-particle δ functions (which give the probability densities at particle coalescence points) as well as the mass–velocity, Darwin, and orbit–orbit Hamiltonians for all states and systems considered in this work. The quantities in this table depend neither on how the spins of the electrons and positron are added nor on the value of the total angular-momentum quantum number J. A useful reference value for the electron-positron contact densities listed in Table III is that of the positronium atom, which can be evaluated analytically and is $\langle \delta_{e^- e^+} \rangle = 1/(8\pi) \approx 0.039\,789$ a.u. One can see that the corresponding entries in Table III are considerably smaller than this value. This indicates that even in the triplet states, where the Ps + Be$^+$ configuration dominates, the Ps atom "orbiting" the ion is rather loose due to its interaction with the latter.

In Table IV we show the expectation values of the Fermi contact interaction, given by Eq. (16), for all systems and states considered in this work. Note that for positronic beryllium the expectation values have different magnitude depending on the total (electrons + positron) spin quantum number S. For the quartet states $\langle \mathcal{H}_{\text{SSF}} \rangle$ they are about 1%–2% larger than for the doublet states.

Table V shows the expectation values of the annihilation channel interaction [$\mathcal{H}_A$ in Eq. (21)], which is present only in systems containing a positron. As expected, the magnitude of $\langle \mathcal{H}_A \rangle$ in the quartet states is much larger (roughly by a factor of four) than in the doublet states. This notable difference is easy to understand: the factor $3/4 + s'_i s_j$ that is present in Eq. (21) vanishes for a positron-electron pair if the spins of the particles in this pair add up to zero.

The mean values of J-dependent operators for the e^+[Be]($^{2;3}P$) and e^+[Be]($^{4;3}P$) states are given in Table VI. One can note that the spin-same-orbit term $\langle \mathcal{H}_{\text{SO1}} \rangle$ is largely (by about 70%) canceled out by the spin-other-orbit term $\langle \mathcal{H}_{\text{SO2}} \rangle$. The corresponding fine-structure splitting diagram is shown in Fig. 1. One can see that the contribution of the noncontact spin–spin interaction energy, E_{SSN}, to the fine-structure splitting is significantly smaller than that of the spin-orbit interaction energy E_{SO}. This situation is similar to

what occurs in the lowest triplet P state of neutral beryllium [67]. Another thing to note is that even after the inclusion of the fine-structure splitting the energy levels of the quartet state ($^{4;3}P$) still remain higher than those for the doublet state ($^{2;3}P$).

The total energies of the states under consideration are calculated as follows:

$$E_{\text{TOT}} = E_{\text{NR}} + \alpha^2 \left(E_{\text{REL}}^{\text{shift}} + E_{\text{SO}} + E_{\text{SSN}} \right), \qquad (39)$$

where

$$E_{\text{REL}}^{\text{shift}} = E_{\text{MV}} + E_{\text{D}} + E_{\text{OO}} + E_{\text{SSF}} + E_{\text{A}} \qquad (40)$$

is the part of the relativistic correction $E_{\text{REL}}^{(2)}$ that uniformly shifts the entire manifold of fine-structure levels and

$$E_{\text{SO}} = \langle \mathcal{H}_{\text{SO}} \rangle_J, \quad E_{\text{SSN}} = \langle \mathcal{H}_{\text{SSN}} \rangle_J. \qquad (41)$$

In the last two expressions, $\langle \ldots \rangle_J$ stands for the J-dependent average given by Eq. (31).

It is interesting to compare the values of J-dependent relativistic corrections for the e^+[^{9}Be]($^{2,4;3}P$) states with those for the neutral ^{9}Be(^3P) calculated in the ECG basis by Stanke *et al.* [69]. They obtained the values of 0.302760, −0.208909, and 0.002561 a.u. for SO1, SO2, and SSN corrections, respectively (we excluded the factor of α^2 from their data). These values are about 2.1–2.2 times greater than the one for the e^+[^{9}Be]($^{4;3}P$) state and about 3.1–3.2 times greater than the one for the e^+[^{9}Be]($^{2;3}P$) state. Overall, the significantly smaller magnitude of J-dependent relativistic corrections for positronic beryllium in the P state can be explained by the fact that the parent state for this system is Be$^+$(^2S) + Ps. Thus, the orbital angular momentum in e^+[Be]($^{2,4;3}P$) comes largely from the outer electron and positron that are much further away from the three inner electrons and nucleus than it is in the neutral beryllium Be(^3P). Also, the opposite charges of the outer electron and positron forming the Ps atom may cause a partial cancellation of the corresponding contributions to E_{SO1}.

Tables VII and VIII contain the convergence of total relativistic correction, $\alpha^2 \langle \mathcal{H}_{\text{REL}} \rangle$, for the S and P states of the systems considered in this work, respectively. As one can see, the quantities are well converged. Specifically, for all states of the positronic beryllium all values are converged to within five figures after the decimal point, i.e., the estimated accuracy of the total relativistic correction is around 10^{-8} hartree or better.

TABLE VIII. Convergence of total relativistic correction $\alpha^2 \langle \mathcal{H}_{\text{REL}} \rangle$ with the number of basis functions $\mathcal{K}$. All values are in $m$hartree.

$\mathcal{K}$	$e^+[\text{Be}](^{2;3}P_{1/2})$	$e^+[\text{Be}](^{2;3}P_{3/2})$	$e^+[\text{Be}](^{4;3}P_{1/2})$	$e^+[\text{Be}](^{4;3}P_{3/2})$	$e^+[\text{Be}](^{4;3}P_{5/2})$
			^{9}Be		
500	−2.316 227	−2.311 324	−2.305 490	−2.303 671	−2.299 229
1000	−2.318 660	−2.313 894	−2.307 399	−2.305 597	−2.301 299
2000	−2.319 470	−2.314 797	−2.307 960	−2.306 182	−2.301 973
3000	−2.319 509	−2.314 854	−2.307 959	−2.306 185	−2.301 994
4000	−2.319 558	−2.314 913	−2.307 989	−2.306 217	−2.302 036
5000	−2.319 552	−2.314 911	−2.307 973	−2.306 202	−2.302 024
6000	−2.319 553	−2.314 915	−2.307 967	−2.306 197	−2.302 022
			$^\infty$Be		
6000	−2.319 465	−2.314 825	−2.307 881	−2.306 110	−2.301 934

Tables IX and X contain the main results of the paper: the total energies of the positronic complexes, their parent systems, and positron binding energies. One can observe that the inclusion of relativistic corrections only slightly lowers the positron binding energy for all considered states. The effect is less significant for S states, where the change is within 0.5%. For P states, the magnitude of the change is more notable and ranges from 0.6% to 2.2%. Such a small change in the positron binding energy is attributed to nearly complete cancellation of the relativistic effects in any specific state of the positronic beryllium and its parent system. From Tables VII and VIII one can see that the total relativistic correction for all systems is around −2.3 $m$hartree, which is comparable in magnitude to the positron binding energies given in Table X (1.1–3.2 $m$hartree). Yet by far the largest contribution to the relativistic correction, which is due to $\mathcal{H}_{\text{MV}}$ and $\mathcal{H}_{\text{D}}$ interactions, comes from the inner-shell electrons, whose states

remain essentially unaltered when the atom binds a positron. The somewhat larger relative change of the positron binding energies for the P-states of $e^+[\text{Be}]$ takes place because there is no cancellation in the spin-orbit interaction [there is no spin-orbit interaction in the parent system, $\text{Be}^+(^2S)$]. However, the magnitude of the spin–orbit interaction alone in P-states of $e^+[\text{Be}]$ is rather small and it is insufficient to cause any qualitative change.

C. Lifetimes

From an experimental perspective it is crucial to estimate the lifetimes of the positronic complexes. We use the semi-empirical scheme [14,68,70] to calculate the annihilation rates of the positronic complexes with the emission of two or three photons:

$$\Gamma_{2\gamma} = 8\pi D_0 \langle \delta_{e^- e^+, 0} \rangle, \quad \Gamma_{3\gamma} = 8\pi D_1 \langle \delta_{e^- e^+, 1} \rangle, \quad (42)$$

where D_0, D_1 are the two- and three-photon annihilation rates of para- and ortho-positronium, respectively. Indices 0 and 1 here stand for the relative spin of the annihilating electron-positron pair.

TABLE IX. Total relativistic energies (in hartree) of all systems and states considered in the present work. The included uncertainties are due to the basis-size truncation.

State	Energy
^{9}Be(^1S)	−14.668 795 828(1)
$^\infty$Be(^1S)	−14.669 716 725(1)
^{9}Be$^+$(^2S)	−14.326 190 029(1)
$^\infty$Be$^+$(^2S)	−14.327 089 623(1)
$e^+[^9\text{Be}](^{2;1}S)$	−14.672 046(1)
$e^+[^\infty\text{Be}](^{2;1}S)$	−14.672 964(1)
$e^+[^9\text{Be}](^{2;3}S)$	−14.579 326(4)
$e^+[^\infty\text{Be}](^{2;3}S)$	−14.580 228(4)
$e^+[^9\text{Be}](^{4;3}S)$	−14.579 310(4)
$e^+[^\infty\text{Be}](^{4;3}S)$	−14.580 211(4)
$e^+[^9\text{Be}](^{2;3}P_{1/2})$	−14.577 313(9)
$e^+[^\infty\text{Be}](^{2;3}P_{1/2})$	−14.578 214(9)
$e^+[^9\text{Be}](^{2;3}P_{3/2})$	−14.577 309(9)
$e^+[^\infty\text{Be}](^{2;3}P_{3/2})$	−14.578 210(9)
$e^+[^9\text{Be}](^{4;3}P_{1/2})$	−14.577 302(9)
$e^+[^\infty\text{Be}](^{4;3}P_{1/2})$	−14.578 203(9)
$e^+[^9\text{Be}](^{4;3}P_{3/2})$	−14.577 300(9)
$e^+[^\infty\text{Be}](^{4;3}P_{3/2})$	−14.578 201(9)
$e^+[^9\text{Be}](^{4;3}P_{5/2})$	−14.577 296(9)
$e^+[^\infty\text{Be}](^{4;3}P_{5/2})$	−14.578 197(9)

TABLE X. Nonrelativistic (ϵ_{NR}) and relativistic (ϵ_{REL}) positron binding energies (in $m$hartree) for different states of positronic beryllium.

$e^+[\text{A}]$(state)	ϵ_{NR}	ϵ_{REL}
$e^+[^9\text{Be}](^{2;1}S)$	3.256(1)	3.250(1)
$e^+[^\infty\text{Be}](^{2;1}S)$	3.254(1)	3.247(1)
$e^+[^9\text{Be}](^{2;3}S)$	3.137(5)	3.136(5)
$e^+[^\infty\text{Be}](^{2;3}S)$	3.138(5)	3.138(5)
$e^+[^9\text{Be}](^{4;3}S)$	3.137(5)	3.120(5)
$e^+[^\infty\text{Be}](^{4;3}S)$	3.138(5)	3.121(5)
$e^+[^9\text{Be}](^{2;3}P_{1/2})$	1.130(9)	1.123(9)
$e^+[^\infty\text{Be}](^{2;3}P_{1/2})$	1.132(9)	1.125(9)
$e^+[^9\text{Be}](^{2;3}P_{3/2})$	1.130(9)	1.119(9)
$e^+[^\infty\text{Be}](^{2;3}P_{3/2})$	1.132(9)	1.120(9)
$e^+[^9\text{Be}](^{4;3}P_{1/2})$	1.130(9)	1.112(9)
$e^+[^\infty\text{Be}](^{4;3}P_{1/2})$	1.132(9)	1.113(9)
$e^+[^9\text{Be}](^{4;3}P_{3/2})$	1.130(9)	1.110(9)
$e^+[^\infty\text{Be}](^{4;3}P_{3/2})$	1.132(9)	1.111(9)
$e^+[^9\text{Be}](^{4;3}P_{5/2})$	1.130(9)	1.106(9)
$e^+[^\infty\text{Be}](^{4;3}P_{5/2})$	1.132(9)	1.107(9)

TABLE XI. Spin-dependent expectation values $\langle \bar{\delta}_{e^- e^+} \rangle$ (in a.u.), average lifetimes τ (in ns), and averaged annihilation rates $\Gamma_{2\gamma,\mathrm{av}}$ (in μs^{-1}) of the positronic complexes considered in this work.

$e^+[A]$(state)	Ref.	$\langle \bar{\delta}_{e^- e^+,0} \rangle$	$\langle \bar{\delta}_{e^- e^+,1} \rangle$	τ	$\Gamma_{2\gamma,\mathrm{av}}$
$e^+[^9\mathrm{Be}](2^{;1}S)$	This work	$2.1616(2) \times 10^{-3}$	$6.4847(5) \times 10^{-3}$	$2.2979(1)$	$434.04(4)$
$e^+[^9\mathrm{Be}](2^{;1}S)$	Ref. [14]	2.140×10^{-3}	6.419×10^{-3}	2.321	429.7
$e^+[^9\mathrm{Be}](2^{;3}S)$	This work	$2.1397(3) \times 10^{-2}$	$7.134(1) \times 10^{-3}$	$0.23268(3)$	$1432.3(2)$
$e^+[^9\mathrm{Be}](2^{;3}S)$	Ref. [14]	2.134×10^{-2}	7.12×10^{-3}	0.2333	1428
$e^+[^9\mathrm{Be}](4^{;3}S)$	This work	$7.36(7) \times 10^{-7}$	$2.8531(4) \times 10^{-2}$	$192.46(3)$	
$e^+[^9\mathrm{Be}](4^{;3}S)$	Ref. [14]	6.4×10^{-7}	2.846×10^{-2}	193.2	
$e^+[^9\mathrm{Be}](2^{;3}P)$	This work	$1.545(1) \times 10^{-2}$	$5.171(4) \times 10^{-3}$	$0.3222(2)$	$1035(1)$
$e^+[^9\mathrm{Be}](4^{;3}P)$	This work	$7.62(3) \times 10^{-7}$	$2.061(1) \times 10^{-2}$	$193.2(2)$	

The values of D_i ($i = 1, 2$) are obtained in QED as an expansion in α:

$$D_i = D_i^{(0)}[1 + A_i \alpha + B_i \alpha^2 + \cdots], \qquad (43)$$

where $D_i^{(0)}$ is the leading-order annihilation rate, and $A_i, B_i, \ldots$ are the coefficients of the expansion. The expressions for $D_i^{(0)}$ (in a.u.) are the following:

$$D_0^{(0)} = \frac{\alpha^5}{2}, \quad D_1^{(0)} = \frac{2(\pi^2 - 9)\alpha^6}{9\pi}. \qquad (44)$$

We used the value of D_0 from Ref. [71], evaluated up to the order of $\alpha^3 \ln^2(\alpha)$: $D_0 = 7989.50(2)\ \mu s^{-1}$, and D_1 from Ref. [72], evaluated up to $\alpha^3 \ln(\alpha)$: $D_1 = 7.039979(11)\ \mu s^{-1}$.

The expectation values in (42) are calculated as follows:

$$\langle \delta_{e^- e^+,0} \rangle = \langle \Psi | \sum_{i=1}^{n_e} | \chi_{i0} \rangle \delta(r_{e^+ i}) \langle \chi_{i0} | | \Psi \rangle, \qquad (45)$$

$$\langle \delta_{e^- e^+,1} \rangle = \langle \Psi | \sum_{j=1}^{3} \sum_{i=1}^{n_e} | \chi_{ij} \rangle \delta(r_{e^+ i}) \langle \chi_{ij} | | \Psi \rangle, \qquad (46)$$

where the summation over i goes over electrons only and χ_{ij} are spin-pair functions:

$$\chi_{i0} = \frac{1}{\sqrt{2}} [\beta(e^+)\alpha(i) - \alpha(e^+)\beta(i)], \qquad (47)$$

$$\chi_{i1} = \frac{1}{\sqrt{2}} [\beta(e^+)\alpha(i) + \alpha(e^+)\beta(i)], \qquad (48)$$

$$\chi_{i2} = \alpha(e^+)\alpha(i), \quad \chi_{i3} = \beta(e^+)\beta(i). \qquad (49)$$

Note that $\langle \delta_{e^- e^+,0} \rangle + \langle \delta_{e^- e^+,1} \rangle = n_e \langle \delta_{e^- e^+} \rangle$. The average lifetime of a positronic system is calculated as

$$\tau = \frac{1}{\Gamma_{2\gamma} + \Gamma_{3\gamma}}. \qquad (50)$$

We also evaluate the spin-averaged annihilation constant, which is most likely to be measured experimentally:

$$\Gamma_{2\gamma,\mathrm{av}} = \frac{(2S_{\mathrm{high}} + 1)\Gamma_{2\gamma,\mathrm{high}} + (2S_{\mathrm{low}} + 1)\Gamma_{2\gamma,\mathrm{low}}}{2S_{\mathrm{high}} + 2S_{\mathrm{low}} + 2}. \qquad (51)$$

We calculate these quantities and present them in Table XI, where we also make a comparison with the values obtained in Ref. [14] for S states. We note that we use the "drachmanized" values of the δ function expectation values in all calculations in order to improve the accuracy. This makes our numerical

results better converged by around three orders of magnitude than those reported previously in Ref. [14].

Since the main (two-photon) annihilation channel corresponds to the relative spin of the pair being equal to zero, lifetimes of the "high" states, where spin projections of the outer electrons and the positron are the same, are much larger than for the "low" states. This trend can be clearly seen in Table XI. All quartet (total spin) states have the average lifetime around 193 nanoseconds, while for the doublet states they are two to three orders of magnitude shorter, ranging from 0.23 to 2.3 nanoseconds.

IV. CONCLUSION

In the present work we studied three bound states of $e^+[\mathrm{Be}]$: singlet and triplet S states, and the triplet P state. Using the variational method with large expansions in terms of explicitly correlated Gaussian basis functions we accurately determined the nonrelativistic energies, structural properties, and electron–positron annihilation rates of the positronic complexes and its decay products. Then we perturbatively included the leading-order relativistic corrections and calculated the resulting positron binding energies. We showed that taking the leading-order scalar and spin-dependent relativistic effects into account lowers the binding energies of $e^+[\mathrm{Be}]$ by just about 2% or less. Even though in absolute terms the relativistic effects, most notably the scalar ones—the mass–velocity and Darwin, shift the energy levels of all considered states of positronic beryllium quite significantly (the change of around -2.3 *m*hartree is comparable or exceeds the positron binding energies), these effects almost completely cancel out when the difference with the parent system (i.e., positron binding energy) is computed. At the same time, the spin-orbit and noncontact spin–spin effects in the triplet P state of the positronic beryllium, which do not cancel out at all (they vanish in the parent system), are too small in magnitude to alter the positron binding energy significantly. The same applies to the annihilation channel interaction in all considered states of $e^+[\mathrm{Be}]$—while only a small fraction of it is canceled out, it is simply too weak to cause any notable change in the positron binding energies. Therefore, the results of our calculations provide an unambiguous and rigorous theoretical confirmation of the dynamical stability of the above three states of positronic beryllium. We hope that the existence of such positron–atom complexes will be confirmed in future experiments.

[1] J. A. Wheeler, Polyelectrons, Ann. N. Y. Acad. Sci. **48**, 219 (1946).

[2] G. G. Ryzhikh and J. Mitroy, Positronic lithium, an electronically stable Li-e^+ ground state, Phys. Rev. Lett. **79**, 4124 (1997).

[3] K. Strasburger and H. Chojnacki, Quantum chemical study of simple positronic systems using explicitly correlated Gaussian functions – PsH and PsLi$^+$, J. Chem. Phys. **108**, 3218 (1998).

[4] D. M. Schrader, Bound states of positrons with atoms and molecules: Theory, Nucl. Instrum. Methods Phys. Res., Sect. B **143**, 209 (1998).

[5] G. G. Ryzhikh, J. Mitroy, and K. Varga, The structure of exotic atoms containing positrons and positronium, J. Phys. B: At., Mol. Opt. Phys. **31**, 3965 (1998).

[6] J. Mitroy, M. W. J. Bromley, and G. G. Ryzhikh, Positron and positronium binding to atoms, J. Phys. B: At., Mol. Opt. Phys. **35**, R81 (2002).

[7] V. A. Dzuba, V. V. Flambaum, and G. F. Gribakin, Detecting positron-atom bound states through resonant annihilation, Phys. Rev. Lett. **105**, 203401 (2010).

[8] G. F. Gribakin, J. A. Young, and C. M. Surko, Positron-molecule interactions: Resonant attachment, annihilation, and bound states, Rev. Mod. Phys. **82**, 2557 (2010).

[9] X. Cheng, D. Babikov, and D. M. Schrader, Binding-energy predictions of positrons and atoms, Phys. Rev. A **83**, 032504 (2011).

[10] V. A. Dzuba, V. V. Flambaum, G. F. Gribakin, and C. Harabati, Relativistic linearized coupled-cluster single-double calculations of positron-atom bound states, Phys. Rev. A **86**, 032503 (2012).

[11] D. Bressanini, Positron binding to lithium excited states, Phys. Rev. Lett. **109**, 223401 (2012).

[12] S. Bubin and O. V. Prezhdo, Excited states of positronic lithium and beryllium, Phys. Rev. Lett. **111**, 193401 (2013).

[13] C. Harabati, V. A. Dzuba, and V. V. Flambaum, Identification of atoms that can bind positrons, Phys. Rev. A **89**, 022517 (2014).

[14] K. Strasburger, Excited s-symmetry states of positronic lithium and beryllium, J. Chem. Phys. **144**, 144316 (2016).

[15] K. R. Brorsen, M. V. Pak, and S. Hammes-Schiffer, Calculation of positron binding energies and electron-positron annihilation rates for atomic systems with the reduced explicitly correlated Hartree–Fock method in the nuclear-electronic orbital framework, J. Phys. Chem. A **121**, 515 (2017).

[16] T. Yamashita, M. Umair, and Y. Kino, Bound and resonance states of positronic copper atoms, J. Phys. B: At., Mol. Opt. Phys. **50**, 205002 (2017).

[17] P. H. R. Amaral and J. R. Mohallem, Descriptor for positron binding to atoms, Phys. Rev. A **104**, 042808 (2021).

[18] J. A. Charry Martinez, M. Barborini, and A. Tkatchenko, Correlated wave functions for electron-positron interactions in atoms and molecules, J. Chem. Theory Comput. **18**, 2267 (2022).

[19] J. Hofierka, B. Cunningham, C. M. Rawlins, C. H. Patterson, and D. G. Green, Gaussian-basis many-body theory calculations of positron binding to negative ions and atoms, arXiv:2311.13066.

[20] A. P. Mills, Observation of the positronium negative ion, Phys. Rev. Lett. **46**, 717 (1981).

[21] A. P. Mills, Measurement of the decay rate of the positronium negative ion, Phys. Rev. Lett. **50**, 671 (1983).

[22] H. Ceeh, C. Hugenschmidt, K. Schreckenbach, S. A. Gärtner, P. G. Thirolf, F. Fleischer, and D. Schwalm, Precision measurement of the decay rate of the negative positronium ion Ps$^-$, Phys. Rev. A **84**, 062508 (2011).

[23] D. B. Cassidy and A. P. Mills, The production of molecular positronium, Nature (London) **449**, 195 (2007).

[24] D. B. Cassidy, T. H. Hisakado, H. W. K. Tom, and A. P. Mills, Optical spectroscopy of molecular positronium, Phys. Rev. Lett. **108**, 133402 (2012).

[25] D. M. Schrader, F. M. Jacobsen, N.-P. Frandsen, and U. Mikkelsen, Formation of positronium hydride, Phys. Rev. Lett. **69**, 57 (1992).

[26] G. F. Gribakin and C. M. R. Lee, Positron annihilation in molecules by capture into vibrational Feshbach resonances of infrared-active modes, Phys. Rev. Lett. **97**, 193201 (2006).

[27] J. R. Danielson, J. J. Gosselin, and C. M. Surko, Dipole enhancement of positron binding to molecules, Phys. Rev. Lett. **104**, 233201 (2010).

[28] A. C. L. Jones, J. R. Danielson, M. R. Natisin, and C. M. Surko, Role of vibrational dynamics in resonant positron annihilation on molecules, Phys. Rev. Lett. **110**, 223201 (2013).

[29] C. M. Surko, J. R. Danielson, G. F. Gribakin, and R. E. Continetti, Measuring positron-atom binding energies through laser-assisted photorecombination, New J. Phys. **14**, 065004 (2012).

[30] J. Mitroy and G. G. Ryzhikh, Measuring the positron affinities of atoms, J. Phys. B: At., Mol. Opt. Phys. **32**, L411 (1999).

[31] M. W. J. Bromley and J. Mitroy, Configuration-interaction calculations of PsH and e^+Be, Phys. Rev. A **65**, 012505 (2001).

[32] J. Mitroy, Structure of the LiPs and e^+Be systems, J. At. Mol. Sci. **1**, 275 (2010).

[33] M. W. J. Bromley and J. Mitroy, Excited states of positronic atoms, Phys. Rev. A **75**, 042506 (2007).

[34] J. Mitroy, Expectation values of the e^+Li system, Phys. Rev. A **70**, 024502 (2004).

[35] M. W. J. Bromley and J. Mitroy, Positron and positronium interactions with Cu, Phys. Rev. A **66**, 062504 (2002).

[36] J. Mitroy, Positron-atom complexes as quantum halo states, Phys. Rev. Lett. **94**, 033402 (2005).

[37] T. Yamashita and Y. Kino, Relativistic corrections to the binding energy of positronic alkali-metal atoms, Phys. Rev. A **100**, 062511 (2019).

[38] S. F. Boys, The integral formulae for the variational solution of the molecular many-electron wave equations in terms of Gaussian functions with direct electronic correlation, Proc. R. Soc. London, Ser. A **258**, 402 (1960).

[39] K. Singer, The use of Gaussian (exponential quadratic) wave functions in molecular problems. I. General formulae for the evaluation of integrals, Proc. R. Soc. London, Ser. A **258**, 412 (1960).

[40] V. I. Kukulin and V. M. Krasnopol'sky, A stochastic variational method for few-body systems, J. Phys. G: Nucl. Phys. **3**, 795 (1977).

[41] K. Varga and Y. Suzuki, Precise solution of few-body problems with the stochastic variational method on a correlated Gaussian basis, Phys. Rev. C **52**, 2885 (1995).

[42] Y. Suzuki and K. Varga, *Stochastic Variational Approach to Quantum-Mechanical Few-Body Problems*, Lecture Notes in Physics (Springer, Berlin, 1998).

[43] J. Rychlewski, *Explicitly Correlated Wave Functions in Chemistry and Physics: Theory and Applications*, Progress in Theoretical Chemistry and Physics (Kluwer, Dordrecht, 2003).

[44] J. Mitroy, S. Bubin, W. Horiuchi, Y. Suzuki, L. Adamowicz, W. Cencek, K. Szalewicz, J. Komasa, D. Blume, and K. Varga, Theory and application of explicitly correlated Gaussians, Rev. Mod. Phys. **85**, 693 (2013).

[45] S. Bubin, M. Pavanello, W.-C. Tung, K. L. Sharkey, and L. Adamowicz, Born–Oppenheimer and non-Born–Oppenheimer, atomic and molecular calculations with explicitly correlated Gaussians, Chem. Rev. (Washington, DC, U. S.) **113**, 36 (2013).

[46] S. Bubin and L. Adamowicz, Matrix elements of N-particle explicitly correlated Gaussian basis functions with complex exponential parameters, J. Chem. Phys. **124**, 224317 (2006).

[47] S. Bubin and L. Adamowicz, Energy and energy gradient matrix elements with N-particle explicitly correlated complex Gaussian basis functions with $L = 1$, J. Chem. Phys. **128**, 114107 (2008).

[48] M. Hamermesh, *Group Theory and Its Application to Physical Problems* (Addison-Wesley, Reading, 1962).

[49] R. Pauncz, *Spin Eigenfunctions* (Plenum, New York, 1979).

[50] M. Stanke, S. Bubin, and L. Adamowicz, Lowest ten ^1P Rydberg states of beryllium calculated with all-electron explicitly correlated Gaussian functions, J. Phys. B: At., Mol. Opt. Phys. **52**, 155002 (2019).

[51] I. Hornyák, L. Adamowicz, and S. Bubin, Low-lying ^2S states of the singly charged carbon ion, Phys. Rev. A **102**, 062825 (2020).

[52] S. Nasiri, T. Shomenov, S. Bubin, and L. Adamowicz, High-accuracy calculations of the lowest eleven Rydberg ^2P states of Li atom, J. Phys. B: At., Mol. Opt. Phys. **54**, 085003 (2021).

[53] I. Hornyák, S. Nasiri, S. Bubin, and L. Adamowicz, ^2S Rydberg spectrum of the boron atom, Phys. Rev. A **104**, 032809 (2021).

[54] W. E. Caswell and G. P. Lepage, Effective Lagrangians for bound state problems in QED, QCD, and other field theories, Phys. Lett. B **167**, 437 (1986).

[55] K. Pachucki, Effective Hamiltonian approach to the bound state: Positronium hyperfine structure, Phys. Rev. A **56**, 297 (1997).

[56] H. A. Bethe and E. E. Salpeter, *Quantum Mechanics of One- and Two-Electron Atoms* (Plenum, New York, 1977).

[57] A. I. Akhiezer and V. B. Berestetskii, *Quantum Electrodynamics* (John Wiley & Sons, New York, 1965).

[58] J. Hiller, J. Sucher, and G. Feinberg, New techniques for evaluating parity-conserving and parity-violating contact interactions, Phys. Rev. A **18**, 2399 (1978).

[59] R. J. Drachman and J. Sucher, Annihilation in positron-atom collisions: A new approach, Phys. Rev. A **20**, 442 (1979).

[60] J. Hiller, J. Sucher, A. Bhatia, and G. Feinberg, Parity-violating electric-dipole transitions in helium, Phys. Rev. A **21**, 1082 (1980).

[61] R. J. Drachman, A new global operator for two-particle delta functions, J. Phys. B: At. Mol. Phys. **14**, 2733 (1981).

[62] K. Pachucki, W. Cencek, and J. Komasa, On the acceleration of the convergence of singular operators in Gaussian basis sets, J. Chem. Phys. **122**, 184101 (2005).

[63] P. Jeszenszki, R. T. Ireland, D. Ferenc, and E. Mátyus, On the inclusion of cusp effects in expectation values with explicitly correlated Gaussians, Int. J. Quantum Chem. **122**, e26819 (2022).

[64] S. Nasiri, L. Adamowicz, and S. Bubin, Benchmark calculations of the energy spectra and oscillator strengths of the beryllium atom, J. Phys. Chem. Ref. Data **50**, 043107 (2021).

[65] S. Nasiri, J. Liu, S. Bubin, M. Stanke, A. Kȩdziorski, and L. Adamowicz, Oscillator strengths and interstate transition energies involving ^2S and ^2P states of the Li atom, At. Data Nucl. Data Tables **149**, 101559 (2023).

[66] B. R. Judd, *Operator Techniques in Atomic Spectroscopy*, Princeton Landmarks in Mathematics and Physics (Princeton University Press, Princeton, New Jersey, 1998).

[67] A. Kȩdziorski, M. Stanke, and L. Adamowicz, Atomic fine-structure calculations performed with a finite-nuclear-mass approach and with all-electron explicitly correlated Gaussian functions, Chem. Phys. Lett. **751**, 137476 (2020).

[68] D. M. Schrader, Compounds of positrons with koino-atoms and -molecules, in *Physics with many positrons, Proceedings of the International School of Physics "Enrico Fermi,"* edited by A. Dupasquier, A. Mills, and R. Brusa (IOS Press, Amsterdam, 2010), Vol. 174, pp. 77–187.

[69] M. Stanke, A. Kȩdziorski, and L. Adamowicz, Fine structure of the beryllium ^3P states calculated with all-electron explicitly correlated Gaussian functions, Phys. Rev. A **105**, 012813 (2022).

[70] S. Bubin and K. Varga, Ground-state energy and relativistic corrections for positronium hydride, Phys. Rev. A **84**, 012509 (2011).

[71] A. Czarnecki, K. Melnikov, and A. Yelkhovsky, Calculation of α^2 corrections to parapositronium decay, Phys. Rev. A **61**, 052502 (2000).

[72] B. A. Kniehl, A. V. Kotikov, and O. L. Veretin, Orthopositronium lifetime at $O(\alpha)$ and $O(\alpha^3 \ln \alpha)$ in closed form, Phys. Rev. A **80**, 052501 (2009).